

Nonreciprocal acoustic transmission through dynamic multilayer structures

A. Paliovaos^{1,2} and N. Stefanou²

¹Laboratoire d'Acoustique de l'Université du Mans (LAUM), UMR 6613, Institut d'Acoustique - Graduate School (IA-GS), CNRS, Le Mans Université, Le Mans, France

²Section of Condensed Matter Physics, National and Kapodistrian University of Athens, University Campus, GR-157 84 Athens, Greece



(Received 5 April 2022; revised 22 June 2022; accepted 27 June 2022; published 5 July 2022)

A time Floquet transfer-matrix method for the description of acoustic wave propagation through dynamic stratified structures, modulated by another, low-frequency, pump acoustic wave, is reported. The method is applied to a specific example of a GaAs/AlAs periodic superlattice, subject to a spatiotemporal modulation induced by an evanescent pump wave with frequency in the lowest acoustic band gap of the structure. By means of systematic numerical calculations, we provide compelling evidence for the occurrence of significant nonreciprocal transmission of an acoustic signal with frequency in a high-order acoustic band gap, through inelastic multiple-scattering processes. Our results indicate a promising route to design nonreciprocal acoustic devices.

DOI: [10.1103/PhysRevB.106.024101](https://doi.org/10.1103/PhysRevB.106.024101)

I. INTRODUCTION

It has long been known that two simultaneously propagating sound waves interact with each other, generating new frequencies that result from linear combinations of the frequencies of the primary waves [1,2]. This can be thought as a nonlinear effect, coupling the two sound waves, which can lead to useful applications. For example, based on the nonlinear interaction of an intense low-frequency pump acoustic wave with a weak high-frequency acoustic signal, the so-called nonlinear vibroacoustic wave modulation technique was developed for structural damage detection (see, e.g., Ref. [3] and references therein).

It was also pointed out that phononic structures, the properties of which vary periodically in time, could be used for wave switching, for parametric amplification [4,5], and as circulators [6] and can support topologically protected states [7]. Moreover, time-varying media exhibit intriguing transmission properties which arise from the broken time-reversal symmetry. In general, the lack of time invariance of a linear medium can lead to a nonreciprocal acoustic response, which is an essential ingredient in the design of a phonon diode [8], while mechanisms for nonreciprocal acoustic transmission using a nonlinear element combined with an acoustic filter have been proposed as well [9–12].

In recent years, time-varying structures are being widely explored due to their nonreciprocal response. The existence of unidirectional transmission has been predicted for systems with spatiotemporally modulated density or Young's modulus [13–15], as well as for piezophononic [16], piezoelectric [17,18], and magnetophononic media [19,20]. On the experimental side, nonreciprocal effects have been observed in acoustic structures with rotating elements [21] as well as in mass-spring [22] and electromechanical [23] systems with time-modulated stiffness. However, despite the considerable research activity in this field, dynamic layered acoustic composites have received much less attention [24]. In this paper,

taking advantage of the band-gap structure of periodic layered composites, we investigate how a localized temporal modulation, induced by the excitation of an evanescent low-frequency acoustic mode, can interact strongly with a high-frequency acoustic signal incident normally on such a composite, giving rise to significant unidirectional transmission. Owing to its simplicity, the proposed design constitutes a versatile platform for realizing nonreciprocal acoustic devices with similar performance to or even better performance than other alternative systems under realistic, experimentally achievable conditions, due to the acoustic band-gap structure and the facile control of the wave form in conjunction with the strong modulation induced by the vibrating interfaces. Moreover, the structure is easily amenable to nanofabrication and thus offers extended possibilities for operation up to hypersonic frequencies.

Enhanced nonreciprocity is expected if the signal, depending on its direction of incidence, experiences very different coupling with the modulation field. Our proposal to achieve this is to choose both modulation and signal frequencies (Ω and ω , respectively) to be inside acoustic band gaps and, in particular, close to midgaps in order to ensure strong damping [25] and thus very asymmetric overlap in the forward and backward configurations, as shown schematically in Fig. 1. At the same time, the sum and/or difference frequencies, $\omega + \Omega$ and/or $\omega - \Omega$, should be adjusted to lie within passbands, so that the beams produced by first-order inelastic scattering can be efficiently transmitted through the structure. Of course, the modal shape of the fields involved in the interaction process, i.e., modulation and primary incoming and outgoing signal waves, also plays an important role in achieving maximum efficiency.

The remainder of this paper is structured as follows. In Sec. II we present a detailed analysis of our theoretical method. We begin by deriving the governing equation for the eigenmodes of the acoustic field in an infinite medium with a time-varying mass density. Then, we proceed to

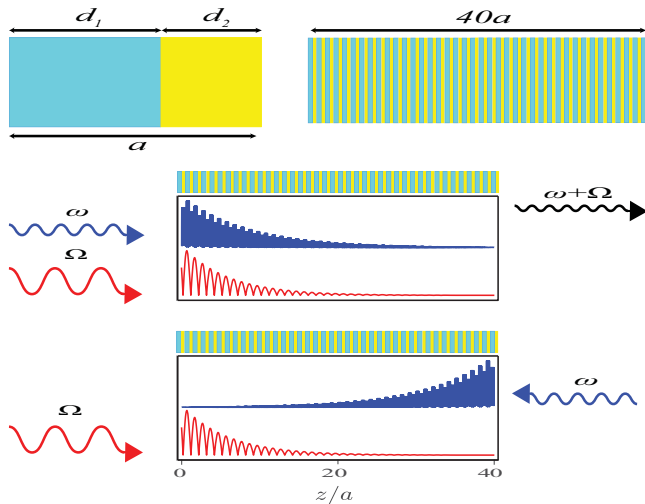


FIG. 1. Schematic description of the asymmetric overlap mechanism for realizing unidirectional transmission through a dynamic one-dimensional periodic composite consisting of a finite sequence of two alternating layers of thickness d_1 and d_2 . A large-amplitude compressional pump acoustic wave of angular frequency Ω within a low-frequency band gap, incident from the left, induces a spatiotemporal modulation localized in the left part of the composite. A second small-amplitude acoustic signal, with angular frequency ω in a high-order band gap, in the time-modulated composite is upconverted in the frequency passband above the gap and transmitted with much higher efficiency when it is incident from the left than when it is incident from the right, because of the asymmetric overlap. This effect can also be realized in the passband below the gap through frequency downconversion.

develop a time Floquet transfer-matrix method for acoustic wave propagation in stratified elastic composites, driven by a low-frequency and high-amplitude pump acoustic wave, including not only the effect of bulk modulation but also the effect of the vibrating interfaces. We also show that, in the limit of zero modulation amplitude, this method is reduced to the usual transfer-matrix formalism for static structures. In Sec. III we apply our method to a specific example of a GaAs/AlAs periodic superlattice, spatiotemporally modulated by an evanescent pump wave with frequency in the lowest acoustic band gap of the structure. Our numerical calculations reveal the occurrence of considerable unidirectional transmission of an acoustic signal with frequency in a high-order acoustic band gap. We present a thorough analysis of our results and provide a consistent interpretation of the underlying physical mechanisms. The last section summarizes the main findings of this paper.

II. THEORY

A. Description of the setup

In this paper we shall be concerned with time-varying stratified structures made of alternating layers of homogeneous and isotropic materials, grown along the z direction. More specifically, we consider a one-dimensional periodic composite consisting of a finite sequence of two alternating layers of thickness d_1 and d_2 , so that $a = d_1 + d_2$ is the lattice

period, as schematically shown in Fig. 1. The layers are characterized by mass densities ρ_1, ρ_2 and Young's moduli E_1, E_2 , respectively. The structure is modulated in space and time by a low-frequency and high-amplitude pump compressional acoustic wave, of angular frequency Ω , incident perpendicular to the layers, and is embedded in an unmodulated (static) host material of mass density ρ_0 and Young's modulus E_0 .

The modulation displacement field, $U(z, t)\hat{\mathbf{z}} = \text{Re}[U(z)\exp(-i\Omega t)]\hat{\mathbf{z}}$, induces a dynamic change in the acoustic response of the structure, first through the vibration of the boundaries of each layer. This translates to a periodic alternation of the mass density and the Young's modulus at a given point z in close vicinity to a vibrating interface. In addition to this interface contribution, the strain field, $\varepsilon(z, t) = \partial U(z, t)/\partial z = \text{Re}[\varepsilon(z)\exp(-i\Omega t)]$, induces a spatiotemporal variation of the bulk density $\Delta\rho(z, t) \simeq -\rho(z)\varepsilon(z, t)$, while changes in the material Young's modulus are neglected as long as we remain in the linear elastic region. Indeed, the mass density along the z axis is given by $\rho(z) = \delta m/(A\delta z)$, where A is the cross-section area and δm is the mass of an infinitesimal slice extending from $z - \delta z/2$ to $z + \delta z/2$. In the presence of a compressional acoustic wave, the slice boundaries (containing the same mass, i.e., atomic planes) are displaced and extend from $z - \delta z/2 + U(z - \delta z/2, t)$ to $z + \delta z/2 + U(z + \delta z/2, t)$. Therefore the slice thickness becomes $\delta z + U(z + \delta z/2, t) - U(z - \delta z/2, t) \simeq \delta z[1 + \varepsilon(z, t)]$, and the mass density reads

$$\rho(z, t) \simeq \rho(z)[1 - \varepsilon(z, t)] = \rho(z)(1 - \bar{\varepsilon}(z)\cos[\Omega t - \phi(z)]), \quad (1)$$

where $\bar{\varepsilon}(z)$ and $\phi(z)$ are the modulus and phase of $\varepsilon(z)$, respectively.

In order to study propagation of a small-amplitude acoustic signal through the *dynamic* structure described above, we subdivide each layer into a sufficiently large number of elementary slices, which can be assumed to be homogeneous, though they vary periodically in time under the influence of the pump field according to Eq. (1) dropping out the dependence on z .

B. Infinite homogeneous medium with a time-varying mass density

We begin our analysis by studying acoustic wave propagation in an infinite, homogeneous time-varying medium, characterized by mass density $\rho(t) = \rho[1 - \bar{\varepsilon}\cos(\Omega t - \phi)]$ according to Eq. (1) and constant Young's modulus E . The parameters $\bar{\varepsilon}, \Omega, \phi$ are determined by the external stimulus which modulates the medium.

The wave equation that describes the space-time evolution of the displacement field $u(z, t)$ and, consequently, wave propagation in this medium reads

$$\begin{aligned} E \frac{\partial^2 u(z, t)}{\partial z^2} &= \frac{\partial}{\partial t} \left[\rho(t) \frac{\partial u(z, t)}{\partial t} \right] \\ &\Rightarrow \frac{\partial^2 u(z, t)}{\partial z^2} - \frac{1}{v^2} [1 - \bar{\varepsilon}\cos(\Omega t - \phi)] \frac{\partial^2 u(z, t)}{\partial t^2} \\ &\quad - \frac{\Omega \bar{\varepsilon}}{v^2} \sin(\Omega t - \phi) \frac{\partial u(z, t)}{\partial t} = 0, \end{aligned} \quad (2)$$

where $v = \sqrt{E/\rho}$. We can seek solutions of the time-periodic equation (2) in the Floquet [26] form

$$u(z, t) = \text{Re} \left[e^{i(kz - \omega t)} \sum_{n=-\infty}^{\infty} w_n e^{in\Omega t} \right] \quad (3)$$

and, substituting into Eq. (2), obtain

$$\begin{aligned} k^2 w_n - \left[\frac{(\omega - n\Omega)}{v^2} \right]^2 w_n \\ + \frac{\bar{\epsilon}}{2v^2} e^{-i\phi} [\omega - (n-1)\Omega] (\omega - n\Omega) w_{n-1} \\ + \frac{\bar{\epsilon}}{2v^2} e^{i\phi} [\omega - (n+1)\Omega] (\omega - n\Omega) w_{n+1} = 0. \end{aligned} \quad (4)$$

This is an eigenfunction-eigenvalue equation of a tridiagonal matrix, which can be solved by standard numerical methods. In this equation, k^2 is the eigenvalue, while the angular frequencies of the pump wave and the incident signal, Ω and ω , respectively, are tunable parameters. Obviously, a monochromatic signal, incident on a periodically time-varying medium, excites polychromatic modes of the form of Eq. (3). The propagation direction of the different (polychromatic) wave modes is determined by the corresponding time-averaged Poynting vector

$$\langle P \rangle = \lim_{\tau \rightarrow \infty} \frac{1}{\tau} \int_0^\tau dt \left[-E \frac{\partial u(z, t)}{\partial z} \frac{\partial u(z, t)}{\partial t} \right], \quad (5)$$

which yields

$$\langle P \rangle = \frac{Ek}{2} \sum_{n=-\infty}^{\infty} |w_n|^2 (\omega - n\Omega). \quad (6)$$

As in the static case, if $\langle P \rangle$ is positive (negative), then the wave is propagating forward (backward). It is worth noting that, since the eigenvalues of Eq. (4) are equal to k^2 , the eigenmodes of the acoustic field in the homogeneous time-varying medium appear in pairs of counterpropagating polychromatic plane waves, with wave numbers $\pm k$, associated with the same eigenvector.

C. Interfaces between homogeneous time-varying media

The most general form of the displacement field in a slab, s , of a homogeneous time-varying medium can be written as a linear combination of the Floquet eigenmodes, given by Eq. (3), which are labeled by an index p

$$\begin{aligned} u_s(z, t) = \sum_{p=-\infty}^{\infty} \text{Re} \left\{ [u_{s;p}^+ e^{ik_{s;p}(z-z_s)} + u_{s;p}^- e^{-ik_{s;p}(z-z_s)}] \right. \\ \left. \times \sum_{n=-\infty}^{\infty} w_{sn;p} e^{-i(\omega - n\Omega)t} \right\}, \end{aligned} \quad (7)$$

where $k_{s;p}$ corresponds to a forward-propagating mode and therefore $-k_{s;p}$ refers to a backward-propagating one, $u_{s;p}^\pm$ are the corresponding amplitudes, and $w_{sn;p}$ are the components of the normalized eigenvector, while z_s is a point inside slab s , around which the displacement field is expanded. With $p = 0$ we label the eigenvalue for which the absolute difference of $k_{s;p}$ from $k = \omega/v$ is smallest, and with $p < 0$ ($p > 0$) we label the eigenvalues with increasing absolute difference which are greater (smaller) than $k = \omega/v$.

At an interface, at z_0 , between two different media, the boundary conditions of continuity of the displacement and the stress fields read

$$\begin{aligned} u_s(z_0, t) = u_{s+1}(z_0, t), \\ E_s \frac{\partial u_s(z, t)}{\partial z} \Big|_{z_0} = E_{s+1} \frac{\partial u_{s+1}(z, t)}{\partial z} \Big|_{z_0}. \end{aligned} \quad (8)$$

However, in this paper, because of the dynamic modulation, the interface oscillates with an angular frequency Ω . If $\Omega \ll \omega$, which is the case that we consider in this paper, the position of the interface does not vary substantially within a period $2\pi/\omega$ of the acoustic signal. Therefore we can employ Eqs. (8) with z_0 replaced by $z_0 + \xi \cos(\Omega t - \theta)$, where ξ and θ are the modulus and phase of $U(z_0)$, respectively, and the first equation in (8), with the help of Eq. (7), yields

$$\begin{aligned} \sum_{p,n=-\infty}^{\infty} [u_{s;p}^+ e^{ik_{s;p}d_s} e^{ik_{s;p}\xi \cos(\Omega t - \theta)} + u_{s;p}^- e^{-ik_{s;p}d_s} e^{-ik_{s;p}\xi \cos(\Omega t - \theta)}] w_{sn;p} e^{-i(\omega - n\Omega)t} \\ = \sum_{p,n=-\infty}^{\infty} [u_{s+1;p}^+ e^{-ik_{s+1;p}d_{s+1}} e^{ik_{s+1;p}\xi \cos(\Omega t - \theta)} + u_{s+1;p}^- e^{ik_{s+1;p}d_{s+1}} e^{-ik_{s+1;p}\xi \cos(\Omega t - \theta)}] w_{s+1n;p} e^{-i(\omega - n\Omega)t}, \end{aligned}$$

where $d_s = |z_0 - z_s|$ and $d_{s+1} = |z_0 - z_{s+1}|$.

Taking advantage of the Jacobi-Anger identity

$$e^{ia \cos \theta} = \sum_{m=-\infty}^{\infty} i^m J_m(a) e^{im\theta},$$

where $J_m(a)$ is the m th Bessel function of the first kind [27], we have

$$\begin{aligned} \sum_{p,n,m=-\infty}^{\infty} [e^{ik_{s;p}d_s} J_m(k_{s;p}\xi) u_{s;p}^+ + e^{-ik_{s;p}d_s} J_m(-k_{s;p}\xi) u_{s;p}^-] i^m e^{-im\theta} w_{sn;p} e^{i(m+n)\Omega t} \\ = \sum_{p,n,m=-\infty}^{\infty} [e^{-ik_{s+1;p}d_{s+1}} J_m(k_{s+1;p}\xi) u_{s+1;p}^+ + e^{ik_{s+1;p}d_{s+1}} J_m(-k_{s+1;p}\xi) u_{s+1;p}^-] i^m e^{-im\theta} w_{s+1n;p} e^{i(m+n)\Omega t}. \end{aligned}$$

This equation must be valid at any moment of time t . Setting $n' = n + m$ and introducing the coefficients

$$\begin{aligned} a_{n';p}^{\pm} &= e^{\pm i k_s p d_s} \sum_{n=-\infty}^{\infty} i^{n'-n} e^{-i(n'-n)\theta} J_{n'-n}(\pm k_s p \xi) w_{sn;p}, \\ b_{n';p}^{\pm} &= e^{\mp i k_{s+1;p} d_{s+1}} \sum_{n=-\infty}^{\infty} i^{n'-n} e^{-i(n'-n)\theta} J_{n'-n}(\pm k_{s+1;p} \xi) w_{s+1n;p}, \end{aligned} \quad (9)$$

we finally obtain

$$\sum_{p=-\infty}^{\infty} [a_{n';p}^+ u_{s;p}^+ + a_{n';p}^- u_{s;p}^-] = \sum_{p=-\infty}^{\infty} [b_{n';p}^+ u_{s+1;p}^+ + b_{n';p}^- u_{s+1;p}^-], \quad \forall n'. \quad (10)$$

Correspondingly, from the continuity of the stress field, we obtain

$$\sum_{p=-\infty}^{\infty} [A_{n';p}^+ u_{s;p}^+ + A_{n';p}^- u_{s;p}^-] = \sum_{p=-\infty}^{\infty} [B_{n';p}^+ u_{s+1;p}^+ + B_{n';p}^- u_{s+1;p}^-], \quad \forall n', \quad (11)$$

where $A_{n';p}^{\pm} = \pm E_s k_s p a_{n';p}^{\pm}$ and $B_{n';p}^{\pm} = \pm E_{s+1} k_{s+1;p} b_{n';p}^{\pm}$. We remind the reader that the presence of Bessel functions in the above formulas, while directly resulting from the Jacobi-Anger identity, is also a staple of frequency modulation tutorials in signal theory [28].

Equations (10) and (11) can be cast in the matrix form

$$\begin{pmatrix} \mathbf{a}^+ & \mathbf{a}^- \\ \mathbf{A}^+ & \mathbf{A}^- \end{pmatrix} \begin{pmatrix} \mathbf{u}_s^+ \\ \mathbf{u}_s^- \end{pmatrix} = \begin{pmatrix} \mathbf{b}^+ & \mathbf{b}^- \\ \mathbf{B}^+ & \mathbf{B}^- \end{pmatrix} \begin{pmatrix} \mathbf{u}_{s+1}^+ \\ \mathbf{u}_{s+1}^- \end{pmatrix}, \quad (12)$$

from which the dynamic transfer matrix \mathbf{T} can be readily defined:

$$\begin{pmatrix} \mathbf{u}_{s+1}^+ \\ \mathbf{u}_{s+1}^- \end{pmatrix} = \mathbf{T} \begin{pmatrix} \mathbf{u}_s^+ \\ \mathbf{u}_s^- \end{pmatrix}, \quad \mathbf{T} = \begin{pmatrix} \mathbf{b}^+ & \mathbf{b}^- \\ \mathbf{B}^+ & \mathbf{B}^- \end{pmatrix}^{-1} \begin{pmatrix} \mathbf{a}^+ & \mathbf{a}^- \\ \mathbf{A}^+ & \mathbf{A}^- \end{pmatrix}. \quad (13)$$

In practice, we truncate the Fourier series to a finite number of terms $n' = \{-N, \dots, 0, \dots, N\}$. Therefore we have $p = \{-N, \dots, 0, \dots, N\}$ Floquet eigenmodes, and \mathbf{T} is a $2(2N+1) \times 2(2N+1)$ square matrix. The value of N is determined by requiring convergence of the solution. In this paper, $\bar{\varepsilon}$, ξ are small, and thus the convergence is very fast.

In the absence of time modulation ($\bar{\varepsilon} = 0$), Eq. (4) yields

$$k_p = \pm \left(\frac{\omega - p\Omega}{v} \right)^2, \quad w_{n;p} = \delta_{np},$$

which expresses frequency invariance of monochromatic waves in a static medium. At an interface between two such media, s and $s+1$, since $\xi = 0$, taking into account the property of Bessel functions $J_{n'-n}(0) = \delta_{n'n}$, it is straightforward to show that the matrices \mathbf{a}^{\pm} , \mathbf{b}^{\pm} , \mathbf{A}^{\pm} , and \mathbf{B}^{\pm} defined above are diagonal. In this case, the linear system (13) of $2(2N+1)$ coupled equations is reduced to $2N+1$ independent 2×2 linear systems

$$\begin{aligned} e^{i k_s p} u_{s;p}^+ + e^{-i k_s p} u_{s;p}^- &= e^{-i k_{s+1;p}} u_{s+1;p}^+ + e^{i k_{s+1;p}} u_{s+1;p}^-, \\ E_s k_s p (e^{i k_s p} u_{s;p}^+ - e^{-i k_s p} u_{s;p}^-) &= E_{s+1} k_{s+1;p} (e^{-i k_{s+1;p}} u_{s+1;p}^+ \\ &\quad - e^{i k_{s+1;p}} u_{s+1;p}^-), \end{aligned} \quad (14)$$

one for each value of $p = \{-N, \dots, 0, \dots, N\}$, which define the usual transfer matrix in the static case.

At an interface between a static and a time-modulated medium, say, with $\bar{\varepsilon}_s = 0$, $\bar{\varepsilon}_{s+1} \neq 0$, and $\xi \neq 0$, the matrices

\mathbf{a}^{\pm} , \mathbf{b}^{\pm} , \mathbf{A}^{\pm} , and \mathbf{B}^{\pm} are nondiagonal, and monochromatic waves of different frequencies are generated due to time modulation and propagate in the static medium. This configuration appears, e.g., when a time-modulated structure is embedded in a static host medium, as we assume in this paper.

At this point, it is essential to stress again the meaning and the role of the different fields discussed in this paper. First, the displacement, $U(z, t)$, and the corresponding strain, $\varepsilon(z, t)$, fields are associated with a pump compressional acoustic wave which, propagating through the static structure, induces a spatiotemporal modulation. On the other hand, the displacement field $u(z, t)$ describes a much-higher-frequency and small-amplitude acoustic signal, which propagates in the modulated layered medium.

The transfer matrix, \mathbf{M} , for the whole structure is obtained by multiplying the transfer matrices of the successive interfaces [29]

$$\mathbf{M} = \prod_{i=1}^{N_i} \mathbf{T}_i \equiv \begin{pmatrix} \mathbf{M}_I & \mathbf{M}_{II} \\ \mathbf{M}_{III} & \mathbf{M}_{IV} \end{pmatrix}, \quad (15)$$

where N_i is the total number of interfaces.

For a monochromatic acoustic wave, incident on the dynamic structure from the left, we obtain the polychromatic transmitted and reflected fields from the equation

$$\begin{pmatrix} \mathbf{u}_{tr} \\ \mathbf{0} \end{pmatrix} = \begin{pmatrix} \mathbf{M}_I & \mathbf{M}_{II} \\ \mathbf{M}_{III} & \mathbf{M}_{IV} \end{pmatrix} \begin{pmatrix} \mathbf{u}_{inc} \\ \mathbf{u}_{rf} \end{pmatrix}, \quad (16)$$

where $\mathbf{u}_{inc} = (0, \dots, 0, u_{inc}, 0, \dots, 0)^T$. Since, as we have already mentioned, the host material is assumed to be unmodulated, the reflected and transmitted monochromatic wave components will propagate independently inside it. Combining the analysis carried out here in Sec. II C with Eq. (6), we obtain the total transmittance and reflectance from the equations

$$\begin{aligned} \mathcal{T} &= \sum_{n=-\infty}^{\infty} \mathcal{T}_n = \sum_{n=-\infty}^{\infty} \left| \frac{u_{tr;n}}{u_{inc}} \right|^2 \left(1 - n \frac{\Omega}{\omega} \right)^2, \\ \mathcal{R} &= \sum_{n=-\infty}^{\infty} \mathcal{R}_n = \sum_{n=-\infty}^{\infty} \left| \frac{u_{rf;n}}{u_{inc}} \right|^2 \left(1 - n \frac{\Omega}{\omega} \right)^2. \end{aligned} \quad (17)$$

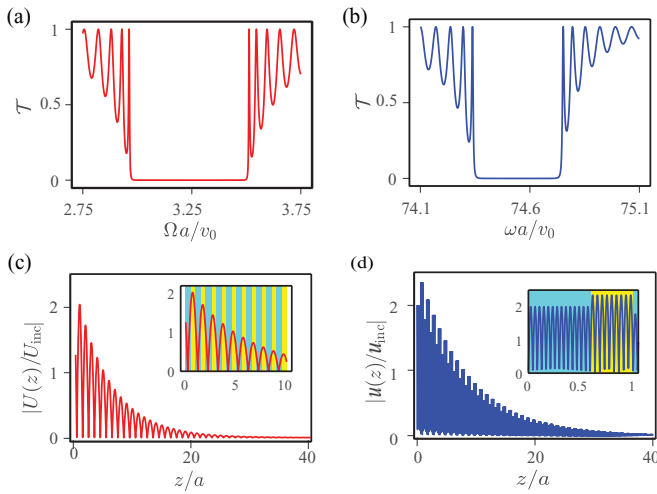


FIG. 2. Transmission spectrum of a one-dimensional periodic acoustic composite, with period a , consisting of an alternating sequence of GaAs and AlAs layers, of thickness $d_1 = 0.6a$ and $d_2 = 0.4a$, respectively, around the lowest-frequency band gap (a) and a high-frequency band gap (b), at normal incidence. The structure has a total length of $40a$ and is embedded in an otherwise homogeneous GaAs material. The amplitude profile of the displacement field, associated with a normally incident acoustic wave of angular frequency $\Omega a/v_0 = 3.435$ and $\omega a/v_0 = 74.68$ (inside these two gaps), is depicted in (c) and (d). Enlarged views in the first ten periods and one period, respectively, are shown in the insets.

III. RESULTS AND DISCUSSION

We shall now apply the method developed in the previous section to a specific example of a periodic layered composite, with its structural unit consisting of two layers of thickness $d_1 = 0.6a$ and $d_2 = 0.4a$, where a is the lattice period. The multilayer structure has a total length of $40a$ and is embedded in an otherwise homogeneous host medium. Examples of such structures, in the nanoscale, are, e.g., semiconductor superlattices, such as Si/Ge [30] or GaAs/AlAs [31–35], or metal/metal superlattices [36–38].

We express all relevant material parameters in dimensionless form, normalized to the corresponding parameters of the host medium (v_0, ρ_0). In this paper we assume $v_1/v_0 = 1$, $v_2/v_0 = 1.0829$, $\rho_1/\rho_0 = 1$, $\rho_2/\rho_0 = 0.7015$, which are appropriate for a GaAs/AlAs superlattice embedded in GaAs [31], while by $\omega a/v_0$ and ka we denote the dimensionless frequency and wave number, respectively.

Periodic acoustic composites exhibit spectral gaps, i.e., frequency regions wherein wave propagation is prohibited [25], due to the destructive interference of the scattered waves, while the magnitude of the gap increases with the contrast of the material parameters. In the case under consideration, taking advantage of the formation of these gaps in the (static) structure, we choose the frequency of the pump wave, Ω , to be inside the lowest-frequency band gap, namely, at $\Omega a/v_0 = 3.435$. The transmission spectrum in the vicinity of the gap is shown in Fig. 2(a). It can be seen that, outside the gap, the transmission exhibits the usual Fabry-Pérot oscillations due to multiple reflections at the surfaces of the sample while,

inside the gap, the transmission is negligibly small because, purposefully, we chose the sample to be relatively thick ($40a$).

Because of the choice of the pump wave frequency inside a band gap, the modulation is induced by an evanescent wave, and only the first few slabs oscillate significantly. The amplitude profile of the corresponding displacement field is depicted in Fig. 2(c).

Reciprocity implies that, in the absence of time modulation, passbands and band gaps of periodic acoustic composites are bidirectional. This means that the acoustic response remains the same when the source and receiver are interchanged. In contrast, when a system is modulated in time, unidirectional band gaps can be formed [13,39], and in this respect, our dynamic structure can support nonreciprocal acoustic transmission. Nevertheless, if the signal has a frequency inside a passband, we have a traveling wave that extends over the entire structure. Therefore the interaction with the dynamic modulation is not radically different when the wave is incident from the left or from the right, even if the modulation is localized at a given surface as we consider in this paper. As a result, only weak nonreciprocal phenomena are expected and indeed observed in this case.

If we want to achieve an enhanced nonreciprocal response, we must take advantage of the localization of the modulation, depicted in Fig. 2(c), and consider an evanescent signal as well. In this case, a left incident wave will propagate only for a few periods and will interact strongly with the dynamic structure which is modulated close to the left boundary. In contrast, if the wave is incident on the structure from the right, it will decay before reaching the left boundary, and only minor interactions will take place since there will be no significant overlap with the modulation. Therefore we choose the frequency of the signal to be inside a high-frequency band gap, namely, that depicted in Fig. 2(b), at $\omega a/v_0 = 74.68$ within the 20th gap. The desired localization of the signal, which indeed undergoes significant decay before it reaches the opposite boundary, is clearly visible in Fig. 2(d). We note that the choice of such a high-order band gap, instead of a lower and probably more robust one, is made in order to ensure the validity of our quasistatic approach to scattering by a vibrating interface ($\Omega \ll \omega$), discussed in Sec. II C.

It is well known from the study of time-varying media [39] that a periodic modulation with angular frequency Ω generates new frequencies. These frequencies, ω_n , differ from that of the incident wave, ω , by $n\Omega$, where $n = \{0, \pm 1, \pm 2, \dots\}$. We recall that we have chosen the signal of frequency ω to be evanescent. Therefore, if it is incident on the structure from the left, a high-amplitude modulation, localized in the vicinity of the left surface, can generate new waves of frequencies ω_n with significant amplitude. Although static and dynamic structures do not share the same transmission spectrum, it would be not unreasonable to expect that some frequency ω_n , if it corresponds to a propagating wave of significant amplitude, can lead to a relatively high transmission coefficient. On the other hand, if the signal is incident on the structure from the right, no strong interaction takes place because of the small overlap with the modulation, and thus no significant propagating waves are expected to be generated.

Nonreciprocity is controlled by the amplitude of the pump wave, $|U_{\text{inc}}|$, which must be high enough in order to have

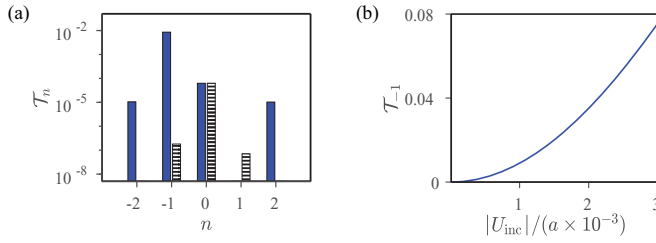


FIG. 3. (a) Relative intensities of the elastic ($n = 0$) and inelastic ($n \neq 0$) transmitted beams, defined by Eq. (17), with respect to the intensity of an acoustic signal incident normally on the periodic composite described in Fig. 2, modulated by a pump acoustic wave with amplitude $|U_{\text{inc}}| = 10^{-3}a$. Both waves (signal and pump) are incident normally on the structure and have frequencies within acoustic band gaps: $\omega a/v_0 = 74.68$ and $\Omega a/v_0 = 3.435$, respectively. Solid (hatched) bars correspond to signal incidence parallel (antiparallel) to that of the pump wave. (b) Variation of the relative intensity of the predominant transmitted beam with the amplitude of the pump wave. The other transmitted beams remain at a relatively low level, as in (a).

a considerable effect. However, this amplitude cannot be arbitrarily large, because the associated high-amplitude strain field may induce inelastic deformations of the materials. Choosing $|U_{\text{inc}}| \sim 10^{-3}a$, the corresponding strain field does not exceed 7×10^{-3} , which is experimentally achievable and ensures that the structure remains in the linear elastic regime [40,41] while, at the same time, causing a significant nonreciprocal response.

It is worth noting that, in view of optimizing the nonreciprocal response for given modulation frequency Ω , the signal frequency ω should be properly adjusted in order to maximize the intensity of a predominant inelastic transmitted beam, keeping all other transmitted beams at a vanishingly low level, as shown in Fig. 3(a). Figure 3(b) shows that the relative intensity of the predominant transmitted beam grows quadratically with the amplitude of the pump wave and can reach 8% under realistic conditions. Different choices of parameters, e.g., geometry, materials, and frequencies, could lead to increased coupling of the primary incoming and outgoing signal waves with the pump field, thus achieving the even higher frequency conversion efficiency that is desirable in practical applications.

If both Ω and ω are inside band gaps, as in the case under consideration, to first order in perturbation theory one expects relatively high transmission of the $n = \pm 1$ inelastic beams, for incidence parallel to that of the pump wave, if $\omega \mp \Omega$, respectively, is within a passband of the static structure. The relevant transmission spectra in the frequency ranges of interest here, for Ω and ω inside the band gaps displayed in Figs. 2(a) and 2(b), are depicted in Figs. 4(a) and 4(b).

On the other hand, in Figs. 4(c) and 4(d) we show the relative intensities of the first-order inelastic transmitted beams, with respect to the intensity of an acoustic signal incident normally on the structure, parallel to a pump acoustic wave with amplitude $U_{\text{inc}} = 10^{-3}a$, in the domain spanned by the pump and signal frequencies. With the dashed lines we represent the equation $\omega - \Omega = \omega_1^-$ in Fig. 4(c) and the equations $\omega + \Omega = \omega_1^+$ and $\omega + \Omega = \omega_2^+$ in Fig. 4(d), where ω_1^\mp

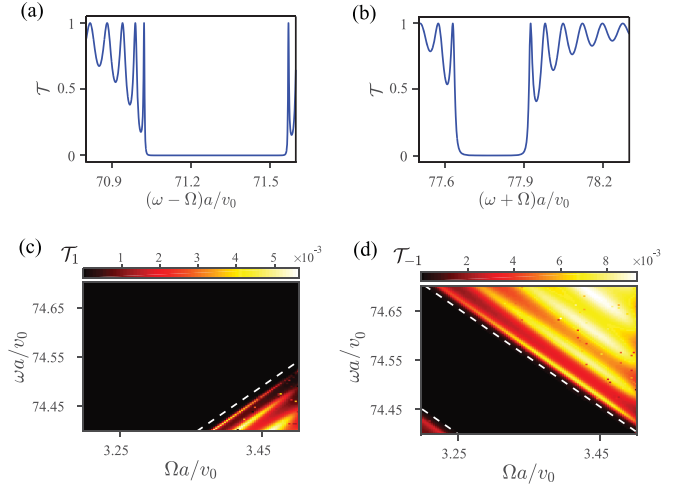


FIG. 4. Transmission spectra of the static, periodic acoustic composite described in Fig. 2, below (a) and above (b) the signal frequencies, at normal incidence. The plotted spectral regions differ from the signal frequencies, ω , by the frequency of the modulation, Ω , that will be applied by a pump wave. (c) and (d) Relative intensities of the first-order inelastic transmitted beams, with respect to the intensity of an acoustic signal incident normally on the structure, parallel to a pump acoustic wave with amplitude $U_{\text{inc}} = 10^{-3}a$, in the domain spanned by the pump and signal frequencies. The dashed lines represent the equation $\omega - \Omega = \omega_1^-$ in (c) and the equations $\omega + \Omega = \omega_1^+$ and $\omega + \Omega = \omega_2^+$ in (d), where by ω_1^\mp and ω_2^\mp we denote the bottom and top, respectively, of the corresponding band gaps, shown in (a) and (b).

and ω_2^\mp denote the bottom and top, respectively, of the corresponding band gaps, shown in Figs. 4(a) and 4(b): $\omega_1^- a/v_0 = 71.03$, $\omega_2^- a/v_0 = 71.55$, $\omega_1^+ a/v_0 = 77.65$, and $\omega_2^+ a/v_0 = 77.90$. It can be readily seen that the regions of total reflection for the dynamic structure coincide with the corresponding band gaps of the static structure. It is also worth noting that the dynamic transmission spectrum follows the Fabry-Pérot oscillations. However, since the pump wave at each frequency Ω induces a different spatiotemporal modulation, the corresponding overlap integral with the initial and final states is different, which explains the variation of the transmittance along a given line of constant frequency $\omega + \Omega$ or $\omega - \Omega$. We note that the borderline $\omega - \Omega = \omega_2^-$ for the onset of inelastic transmission above the band gap in Fig. 4(c) is not visible because it is outside the spectral ranges considered.

Last but not least, it should be pointed out that, as shown by explicit calculations, the effects discussed here are almost entirely due to the vibrating interfaces while the bulk density modulation is negligible, which justifies the neglect of modulation of the homogeneous embedding medium. Therefore, clearly, stratified structures are essential for the manifestation of strong nonreciprocal effects.

IV. CONCLUSIONS

In summary, we developed a time Floquet transfer-matrix method to describe acoustic wave propagation through stratified structures, subject to dynamic modulation by another, low-frequency, pump acoustic wave. Applying this method

to a specific example of a GaAs/AlAs periodic superlattice, under a spatiotemporal modulation induced by an evanescent pump wave with frequency in the lowest acoustic band gap of the structure, we provided evidence for the occurrence of considerable nonreciprocal acoustic effects. More specifically, the simultaneous localization of both pump and signal waves in the vicinity of the same surface of the acoustic composite leads to significant one-way transmission of an evanescent signal at in-gap frequency, when strong inelastic scattering produces a propagating outgoing wave with frequency inside a passband. The proposed design, which takes advantage of the acoustic band-gap structure of periodic elastic composites in order to properly adjust the interaction of the acoustic signal with the dynamic modulation, indicates a promising route to-

wards the realization of nonreciprocal acoustic devices. Other stratified microstructures, which can operate in the linear elastic regime under higher strain fields, will exhibit even better performance. It is worth noting that our results apply to different regions of frequency, provided that the size of the structural units is scaled accordingly. In the high-gigahertz regime that is also relevant to acousto-optics [42,43], nonlinear [44] and phonon damping [45,46] effects, which are not considered in this paper, might play a significant role and influence the device performance.

ACKNOWLEDGMENT

A.P. acknowledges the support from Project No. ExFLEM ANR-21-CE30-0003-01.

-
- [1] A. L. Thuras, R. T. Jenkins, and H. T. O'Neil, *J. Acoust. Soc. Am.* **6**, 173 (1935).
- [2] U. Ingard and D. C. Pridmore-Brown, *J. Acoust. Soc. Am.* **28**, 367 (1956).
- [3] L. Pieczonka, A. Klepka, A. Martowicz, and W. Satszewski, *Opt. Eng.* **55**, 011005 (2016).
- [4] D. W. Wright and R. S. C. Cobbold, *Smart Mater. Struct.* **18**, 015008 (2009).
- [5] D. W. Wright and R. S. C. Cobbold, *Smart Mater. Struct.* **19**, 045006 (2010).
- [6] R. Fleury, D. L. Sounas, C. F. Siek, M. R. Haberman, and A. Alù, *Science* **343**, 516 (2014).
- [7] N. Swintek, S. Matsuo, K. Runge, J. O. Vasseur, P. Lucas, and P. A. Deymier, *J. Appl. Phys. (Melville, NY)* **118**, 063103 (2015).
- [8] A. A. Maznev, A. G. Every, and O. B. Wright, *Wave Motion* **50**, 776 (2013).
- [9] B. Liang, B. Yuan, and J.-C. Cheng, *Phys. Rev. Lett.* **103**, 104301 (2009).
- [10] N. Boechler, G. Theocharis, and C. Daraio, *Nat. Mater.* **10**, 665 (2011).
- [11] F. Li, P. Anzel, J. Y. Yang, P. G. Kevrekidis, and C. Daraio, *Nat. Commun.* **5**, 5311 (2014).
- [12] T. Devaux, V. Tournat, O. Richoux, and V. Pagneux, *Phys. Rev. Lett.* **115**, 234301 (2015).
- [13] G. Trainiti and M. Ruzzene, *New J. Phys.* **18**, 083047 (2016).
- [14] K. Yi, M. Collet, and S. Karkar, *Phys. Rev. B* **96**, 104110 (2017).
- [15] K. Yi, M. Collet, and S. Karkar, *Phys. Rev. B* **98**, 054109 (2018).
- [16] A. Merkel, M. Willatzen, and J. Christensen, *Phys. Rev. Applied* **9**, 034033 (2018).
- [17] C. Croënne, J. O. Vasseur, O. Bou Matar, M.-F. Ponge, P. A. Deymier, A.-C. Hladky-Hennion, and B. Dubus, *Appl. Phys. Lett.* **110**, 061901 (2017).
- [18] C. Croënne, J. O. Vasseur, O. Bou Matar, A.-C. Hladky-Hennion, and B. Dubus, *J. Appl. Phys. (Melville, NY)* **126**, 145108 (2019).
- [19] M. H. Ansari, M. A. Attarzadeh, M. Noh, and M. Amin Karami, *Smart Mater. Struct.* **27**, 015030 (2018).
- [20] J. F. Robillard, O. Bou Matar, J. O. Vasseur, P. A. Deymier, M. Stippinger, A.-C. Hladky-Hennion, Y. Pennec, and B. Djafari-Rouhani, *Appl. Phys. Lett.* **95**, 124104 (2009).
- [21] Q. Wang, Y. Yang, X. Ni, Y. L. Xu, X. C. Sun, Z. G. Chen, L. Feng, X. P. Liu, M. H. Lu, and Y. F. Chen, *Sci. Rep.* **5**, 10880 (2015).
- [22] Y. Wang, B. Yousefzadeh, H. Chen, H. Nassar, G. Huang, and C. Daraio, *Phys. Rev. Lett.* **121**, 194301 (2018).
- [23] J. Marconi, E. Riva, M. Di Ronco, G. Cazzulani, F. Braghin, and M. Ruzzene, *Phys. Rev. Applied* **13**, 031001(R) (2020).
- [24] D. Ramaccia, A. Alù, A. Toscano, and F. Bilotti, *Appl. Phys. Lett.* **118**, 101901 (2021).
- [25] M. M. Sigalas, M. S. Kushwaha, E. N. Economou, M. Kafesaki, I. E. Psarobas, and W. Steurer, *Z. Kristallogr.* **220**, 765 (2005).
- [26] G. Floquet, *Ann. Sci. École Norm. Sup.* **12**, 47 (1883).
- [27] M. Abramowitz and I. E. Stegun, *Handbook of Mathematical Functions with Formulas, Graphs, and Mathematical Tables* (Dover, New York, 1972).
- [28] S. Haykin and M. Moher, *Communication Systems* (Wiley, New York, 2009).
- [29] P. Markoš and C. Soukoulis, *Wave Propagation: From Electrons to Photonic Crystals and Left-Handed Materials* (Princeton University Press, Princeton, 2008).
- [30] H. T. Grahm, H. J. Maris, J. Tauc, and B. Abeles, *Phys. Rev. B* **38**, 6066 (1988).
- [31] C. Colvard, R. Merlin, M. V. Klein, and A. C. Gossard, *Phys. Rev. Lett.* **45**, 298 (1980).
- [32] A. Huynh, B. Perrin, and A. Lematre, *Ultrasonics* **56**, 66 (2015).
- [33] A. Yamamoto, T. Mishina, Y. Masumoto, and M. Nakayama, *Phys. Rev. Lett.* **73**, 740 (1994).
- [34] A. Bartels, T. Dekorsy, H. Kurz, and K. Köhler, *Phys. Rev. Lett.* **82**, 1044 (1999).
- [35] K. Mizoguchi, M. Hase, S. Nakashima, and M. Nakayama, *Phys. Rev. B* **60**, 8262 (1999).
- [36] W. Chen, Y. Lu, H. J. Maris, and G. Xiao, *Phys. Rev. B* **50**, 14506 (1994).
- [37] B. Perrin, B. Bonello, J.-C. Jeannet, and E. Romatet, *Phys. B (Amsterdam)* **219**, 681 (1996).
- [38] C. Rossignol and B. Perrin, *Anal. Sci.* **17**(S4), s245 (2001).
- [39] C. Caloz and Z. Deck-Léger, *IEEE Trans. Antennas Propag.* **68**, 1569 (2020).

- [40] J. Michler, K. Wasmer, S. Meier, and F. Östlund, *Appl. Phys. Lett.* **90**, 043123 (2007).
- [41] S. Wang and P. Pirouz, *Acta Mater.* **55**, 5526 (2007).
- [42] I. E. Psarobas, N. Papanikolaou, N. Stefanou, B. Djafari-Rouhani, B. Bonello, and V. Laude, *Phys. Rev. B* **82**, 174303 (2010).
- [43] E. Almpanis, N. Papanikolaou, and N. Stefanou, *Opt. Express* **22**, 31595 (2014).
- [44] D. Garcia-Pastor, C. Collado, J. Mateu, and R. Aigner, *IEEE Trans. Microwave Theory Tech.* **68**, 1304 (2020).
- [45] W. Chen, H. J. Maris, Z. R. Wasilewski, and S.-I. Tamura, *Philos. Mag. B* **70**, 687 (1994).
- [46] A. A. Maznev, F. Hofmann, A. Jandl, K. Esfarjani, M. T. Bulsara, E. A. Fitzgerald, G. Chen, and K. A. Nelson, *Appl. Phys. Lett.* **102**, 041901 (2013).